Post-print of: Cysewska K., Fernandez L., Jasiński P., Hubin A.: Tailoring the electrochemical degradation of iron protected with polypyrrole films for biodegradable cardiovascular stents. ELECTROCHIMICA ACTA. Vol. 245, (2017), p. 327-336. DOI: 10.1016/j.electacta.2017.05.172

Tailoring the electrochemical degradation of iron protected with polypyrrole films for biodegradable cardiovascular stents

Karolina Cysewska[a,b] Lucía Fernández Macía[b], Piotr Jasi nski[a], Annick Hubin[b]

[a] Faculty of Electronics, Telecommunications and Informatics, Gdansk University of Technology, ul. Narutowicza 11/12, 80-233 Gdansk, Poland
[b] Research group Electrochemical and Surface Engineering, Vrije Universiteit Brussel, Pleinlaan 2, 1050 Brussels, Belgium

A B S T R A C T

The degradation of polypyrrole (PPy) coated iron is studied in phosphate buffer saline solution at 37oC by odd random phase multisine electrochemical impedance spectroscopy (ORP-EIS). PPy is electro-polymerized with anti-inflammatory salicylates incorporated in the film, as a drug release system. The modelling of EIS over time provides the quantitative description of the corrosion behaviour of the material. Thus, the reliable analysis of the degradation stages of PPy coated iron is attained. The outcome of the present study shows that the degradation of iron can be tailored by tuning the properties of the PPy coating for possible medical applications.

Keywords: polypyrrole, iron, corrosion, odd random phase electrochemical, impedance spectroscopy, biodegradable metallic implant

1. Introduction

Nowadays permanent metallic cardiovascular stents are long-term implants [1,2]. The presence of such an implant for long time in human body can cause overgrowth of tissue within the treated portion of the vessel, blockage of the circulatory system and many other clinical complications, such as thrombosis, prolonged physical irritations or chronic inflammation [2,3]. Therefore, in recent years, there is an interest to create biodegradable metallic cardiovascular stents [1–3]. Iron and its alloys are promising materials for this application and have attracted the attention of many researchers [1–6]. Iron possesses very good mechanical properties, similarly to 316L stainless steel (used in permanent cardiovascular stents); it also has favourable biological properties and high biocompatibility [1,2]. However, bare iron degrades too slow on the long term, yet too fast in the initial stages in a physiological media, making it difficult to use in clinical applications [6]. In order to enhance the corrosion rate of iron, the current technology is focused on modifying the iron structure, for example by alloying [6]. Nevertheless, it is also desirable to inhibit its degradation at the initial stages after the implantation. This inhibition will provide a good biocompatibility and an appropriate cell proliferation, which are very crucial during the first days after the implantation [1–3,6].

One promising solution is to modify the surface of the metal with conducting polymer films [7–12].The principal property of these polymers is their metallic-like conductivity due to the conjugated double bond in their backbone [13]. One of the most interesting among the conducting polymers is polypyrrole (PPy) [14–17]. It exhibits high biocompatibility [14], very good stability in different environments [9,15], good adhesion to the substrate [16], excellent electrical, mechanical and thermal properties and high conductivity compared to other conducting polymers [15]. Because of such distinctive properties, PPy has been used in different applications including anti-corrosive coatings [7,8,18,19] and drug release systems [20]. One of the common methods of synthesis on metallic substrates is electrochemical polymerization [21]. This method allows controlling the film properties and provides stronger bonding of the polymer to the substrate compared to a chemical approach [22]. Depending on the polymerization conditions, different morphology, electrical and corrosion properties of the conducting polymer film can be obtained [23]. However, when deposited on an oxidizable metal, an inappropriate selection of the synthesis conditions leads to the dissolution of the substrate, since the potential at which the metal dissolves is much lower than the oxidation potential of the

http://dx.doi.org/10.1016/j.electacta.2017.05.172

monomer. Thus the deposition of the polypyrrole becomes hindered [22,24].Therefore, the choice of the electropolymerization conditions, including the type of electrolyte, is very critical to obtain stable and protective conducting polymer coatings on such kind of metals [7,25].

Polypyrrole has been electropolymerized on several types of oxidizable metals such as magnesium [26], aluminium alloy [27], copper [28], zinc [29], steel and iron [8,19,30–32]. In contrast to the noble metals, such as platinum, where direct deposition of pyrrole occurs [33], non-noble metals seem to require the formation of a stable interface prior to the polymerization. It was shown that in the presence of certain electrolytes, such as oxalic acid [22] or sodium salicylate [8,28], just before the polymer deposition, a passivation layer is formed on the surface of the active metals. This layer blocks the dissolution of the iron substrate and thus provides a stable deposition. It also enhances the adhesion of the polymeric film in the further stages of the electropolymerization [22].

In addition, PPy can be also used to load and release drugs with therapeutic activity, like salicylates [8,9,34], which can be incorporated during the electropolymerization as dopants. Sodium salicylate belongs to the family of non-steroidal, anti-inflammatory agents that reduce pain and fever. During the implant degradation, it could be released into the body, decreasing a possible inflammation caused by the implantation process [9].

The corrosion properties of PPy coatings on different metals have been intensively studied in recent years, for various applications and by utilizing several methods [22,28,34–39]. It was reported that conducting polymers synthesized under certain conditions can prevent the corrosion of certain metals. Bazzaoui et al. studied PPy coated iron in 0.1 M HCl at room temperature using potentiodynamic polarization; they observed the inhibition of the corrosion process by the polypyrrole, synthesized from a solution of saccharin and pyrrole [37]. An improved corrosion protection of steel was also achieved by polypyrrole deposited from a salicylate solution [34]. The protection, assessed by electrochemical impedance spectroscopy in sodium chloride, remained stable up to 20 days.

The mechanism of corrosion protection of iron or steel by a conducting polymer depends on the polymer/metal electrochemical system [28]. In many cases corrosion protection involves a redox reaction (probably catalytic) that forms passivating layer at the metal/polymer interface [28,32,40–42]. In other words, conducting polymer films help to stabilize this layer as a result of galvanic coupling between the coating and the metal [34]. Such mechanism was reported in the case of PPy-salicylates deposited on steel [28], PPy-oxalates on iron [32] or polyaniline (PANI) deposited on steel [41].

In most of the studied cases it is desirable to achieve a stable polymer/metal system with a high corrosion protection of the metal [22,28,34–39]. Yet, for biodegradable metallic stents, the system needs to evolve over time. Besides, it is important to investigate the corrosion and degradation processes of such system under conditions that simulate the human body environment.

In this work, the corrosion performance of differently prepared PPy coatings on iron has been studied at 37 °C in phosphate buffer saline solution (pH 7.4) for the first time. Polypyrrole is electrochemically synthesized in the presence of sodium salicylate, which is incorporated in the coating. The degradation study is performed by odd random phase electrochemical impedance spectroscopy (ORP-EIS) [43–45]. The ORP-EIS data are fitted to the proposed electrical equivalent circuit that represents the electrochemical processes. The parameters that describe the electrochemical system are estimated using a statistically founded method. Besides, the quality of the modelled data is statistically evaluated by confronting the modelling errors against the noise levels. The evolution of the parameters describing the degradation of the PPy/Fe system is obtained. This way, a reliable, quantitative analysis of the behaviour of PPy coated iron in a simulated human body environment is attained. To the best of our knowledge, this subject has not been investigated with this approach before.

2. Experimental

2.1. Chemicals and materials

The following chemicals are used: pyrrole monomer (≥99%, Acros Organics), sodium salicylate (≥99.5%, EMSURE), phosphate buffer saline pH 7.4 (PBS, PanReac AppliChem) containing 2.7 mM KCl, 140 mM NaCl and 10 mM phosphate. The electrolyte for electropolymerization consists of a solution of 0.1 M pyrrole and 0.1 M sodium salicylate. All solutions are made with Mili-Q water.

The substrate is a pure iron plate (≥99.8%, Chempur Feinchemikalien und Forschungsbedarf GmbH).

2.2. Sample treatment

The iron plate is embedded in an epoxy resin. The iron electrode is mechanically grinded with abrasive papers 220, 500 and 1200 SiC grade (Struers), rinsed with ethanol and dried. After the polymerization experiments, the sample is rinsed with Mili-Q water and dried in an N_2 stream.

2.3. PPy film synthesis

The electropolymerization measurements are performed in a one-compartment, three-electrode cell controlled by a Bio-Logic SP-200 potentiostat. The working electrode is the iron with an exposed area of 3.39 cm^2. A $Ag/AgCl_{sat}$ is used as reference electrode and a platinum grid, as counter electrode

The polymer films are electrochemically synthesized on iron in a one step process at 1.2 V vs. $Ag/AgCl_{sat}$ from solution of 0.1 M pyrrole and 0.1 M sodium salicylate, at room temperature. Two coatings, named here PPy_1 and PPy_2, are deposited with the electropolymerization time limited by a specific charge: 6.37 C cm^{-2} for PPy_1 and 2.11 C cm^{-2} for PPy_2.

A preliminary characterization of the corrosion protection of the freshly prepared polymeric films is carried out by potentiodynamic polarization in PBS solution (pH 7.4) at 37 °C from −300 mV to 1 V (vs. OCP) with a 3 mV s^{-1} scan rate. The temperature during the measurements is controlled by a JULABO F12 thermostat.

The film thickness is measured from cross-sectional scanning electron microscope (SEM) images, using JEOL JSM-IT300LV with a tungsten filament source. The thickness of the PPy_1 and PPy_2 coatings is determined to be ∼20 μm and ∼10 μm, respectively (see Supplementary contents, Figure A).

2.4. ORP-EIS measurements

The degradation measurements of PPy_1/Fe and PPy_2/Fe are performed by ORP-EIS during 2 weeks and 1 week, respectively.

The ORP-EIS technique uses an odd random phase multisine as excitation signal. Such signal consists of the sum of harmonically related sine waves with random phases. Only odd harmonics are excited and, per group of 3 consecutive harmonics, one is randomly omitted [43,44]. This allows for the determination of the non-stationarities and non-linearities of the studied system. Every ORP-EIS measurement and its noise distortions are obtained from the calculations of 4 multisine periods. Besides, due to the multisine excitation signal, the measurement time is reduced. The detailed description and explanation of the technique can be found in previous works [44,45].

The measurements are acquired in the 3-electrode cell, water-jacketed at 37 °C, in the PBS solution (pH 7.4). The iron electrode has an exposed area of 0.785 cm^2. The measuring setup consists of a Wenking potentiostat POS 2 (Bank Elektronik) and a National Instrument PCI-4461 DAQ-card with a built-in anti-aliasing filter. The applied multisine signal is digitally composed with MATLAB R2010a software (MathWorks Inc.) MATLAB is also used for processing the collected data and controlling the DAQ-card. The perturbation signal applied is a 3 mV RMS variation around the open circuit potential. The impedance spectrum is acquired in the frequency range of 0.01 Hz–10 kHz.

2.5. Analysis of ORP-EIS data

The data analysis provided by the ORP-EIS technique enable to check whether the impedance data have a good signal-to-noise ratio and fulfil the conditions of stationarity and linearity, necessary for correct experimental impedance data [46].

Equivalent electrical circuits (EEC) are used for modelling the experimental data. The complex modelling residual, which is the difference between the best model and the experiment, is considered to assess the quality of the fit. The EEC modelling is validated based on the following criteria: (1) the model is physically plausible; (2) the modelling residual is low with regard to the noise level; (3) the estimated parameters are physically explicable and have a low standard deviation.

3. Results

3.1. Preliminary electrochemical characterization of PPy/Fe

Prior to the degradation study, the corrosion properties of the PPy_1 and PPy_2 coatings are evaluated by potentiodynamic polarization of the freshly prepared PPy/Fe materials in aqueous solution of PBS (pH 7.4) at 37 °C (Supplementary contents, Figure B). Polarization is commonly used to assess the initial electrochemical properties of metals coated with conducting polymers [32,35]. The corrosion potential and current of both PPy_1/Fe and PPy_2/Fe and bare iron are presented in Table 1. A more noble corrosion potential and a lower corrosion current for the coated iron than for the bare iron indicate that PPy can lower the corrosion rate of iron. Depending on the type of coating, such protection differs; PPy_1 exhibits better corrosion properties compared to the thinner PPy_2 coating. The different corrosion properties observed initially with the polarization measurements anticipate the diverging corrosion behaviour of both coatings. The long term impedance study will enable understanding the electrochemical processes involved.

During the EIS study, the evolution of the open-circuit potential (OCP) is also analysed. The OCP is recorded before each EIS measurement of PPy_1 and PPy_2 coated iron (Fig. 1). For bare iron the evaluation of the OCP is also done for comparison. A sudden drop of the potential can be seen just after the immersion of the electrodes in the PBS solution. Such behaviour can be associated with the ingress of the solution through the polymer pores to the iron surface [39,47,48]. The OCP evolution differs depending on the studied material. In the case of bare iron, after the initial drop, the potential slightly decreases and approximately after 14 h it starts to increase. This is related to the iron passivation process and the formation of different kinds of iron oxides and salts on its surface [32,49]. These inhibit the active corrosion of iron up to approximately 150 h.

Table 1
Corrosion properties of PPy_1/Fe, PPy_2/Fe and bare Fe, evaluated by potentiodynamic polarization.

	PPy_1/Fe	PPy_2/Fe	Bare Fe
E_{corr} vs Ag/$AgCl_{sat}$ [V]	−0.029	−0.25	−0.71
i_{corr} [μA cm^{-2}]	2.46	12.25	14.41

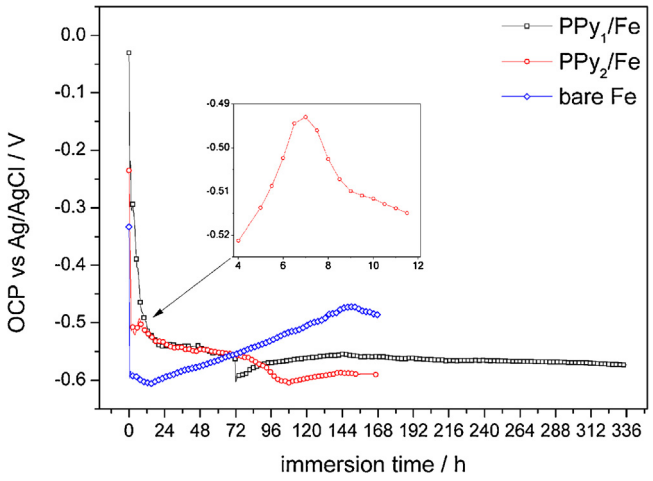

Fig. 1. Evolution of the OCP with time for PPy_1 and PPy_2 coated iron and bare iron in PBS solution (pH 7.4) at 37 °C. Inset: initial increase of the OCP for the PPy_2 coated iron.

The coated iron presents a different behaviour, which, in turn, depends on the characteristics of the coating. The OCP for PPy_1/Fe decreases until approximately 72 h. After this time, it starts to increase and then remains stable up to 2 weeks of immersion (−0.55 V). In the case of the PPy_2 film, the potential after the sudden drop starts to increase up to approximately 7 h (see inset in Fig. 1) and then it decreases with the immersion time. After 144 h of immersion, it reaches a stable value (−0.6 V). The increase of OCP for both types of coatings, suggests that PPy films have certain ability to self-repair [22]. It can be seen that both PPy coatings can provide the protection of the iron until approximately 72 h. Later on, the PPy/Fe materials are more prone to corrode compared to bare iron, which is indicated by a decrease of the OCP. That might imply that PPy coatings are able to enhance the Fe degradation, as it was noted by Rammelt et al. [13]. Based on the OCP analysis, the thinner coating PPy_2, with the worse initial corrosion parameters (E_{corr}, i_{corr}), seems to make the iron more likely to degrade.

3.2. Degradation of PPy/Fe analysed by ORP-EIS

ORP-EIS measurements are performed in order to evaluate the electrochemical degradation of both types of coatings. Figs. 2 and 3 present the ORP-EIS spectra of PPy_1 and PPy_2 coated iron, respectively.

The impedance data clearly show the evolution over time of the PPy/Fe material. Moreover, the EIS behaviour between the PPy_1 and PPy_2 coatings differs. In the case of the PPy_1 coating, the impedance modulus |Z| decreases during the first 50 h, then it evolves steadily until 125 h; after this time the system becomes relatively stable (Fig. 2). For the PPy_2 coating, |Z| decreases from 6 h to 140 h; then a continuous increase of |Z| is seen, particularly at the low frequencies (Fig. 3). The EIS curves suggest that the system may be characterized by three time constants.

3.3. Reliability of the experimental EIS data

The modelling of the experimental EIS data can only be performed if the conditions of linearity and stationarity are met [46]. The quality of the measurements is assessed by the analysis of the levels of noise. In Fig. 4, the experimental curve and noise level

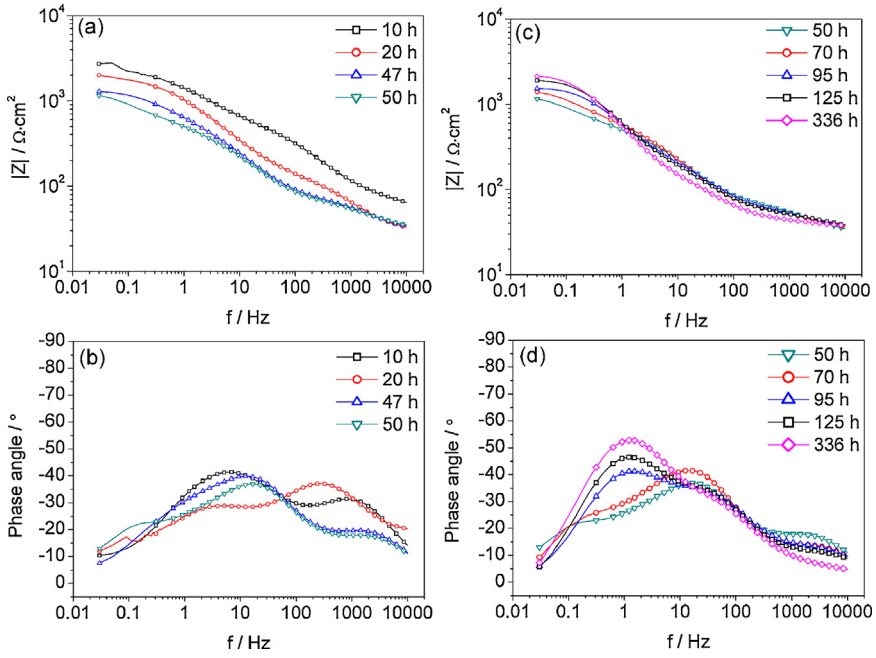

Fig. 2. Bode modulus (a, c) and Bode phase angle (b, d), as a function of immersion time for the PPy_1 coated iron in the PBS solution (pH 7.4) at 37 °C.

are presented together with the modelled curve and modelled residual for selected EIS spectra of the PPy_1/Fe and PPy_2/Fe systems.

It can be seen that all curves related to the noise level, non-stationarities and non-linearities coincide for both systems. Similar characteristics are obtained for the whole dataset recorded. It proves that the EIS data are measured preserving the conditions of linearity and stationarity, which confirms the reliability of the EIS data.

3.4. Modelling of the impedance data: fitting and estimation of the EEC parameters

Once the quality of the experimental data is confirmed, the modelling can be performed. Impedance experiments of PPy_1 and PPy_2 coated iron are modelled using the equivalent electrical circuit in Fig. 5. It is shown together with a scheme of the PPy/Fe system to display the correspondence between the circuit elements and the different layers of the material.

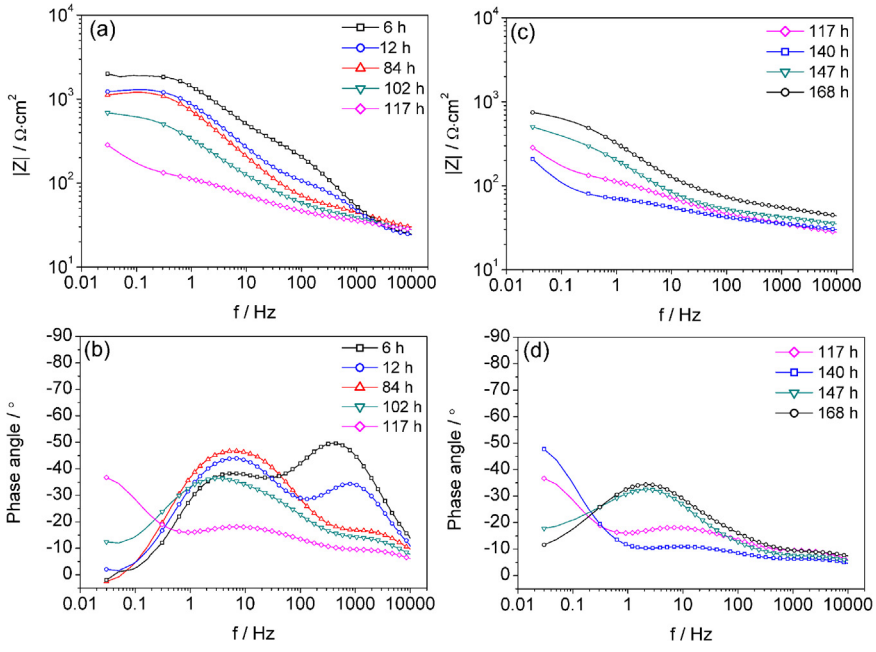

Fig. 3. Bode modulus (a, c) and Bode phase angle (b, d), as a function of immersion time for the PPy_2 coated iron in the PBS solution (pH 7.4) at 37 °C.

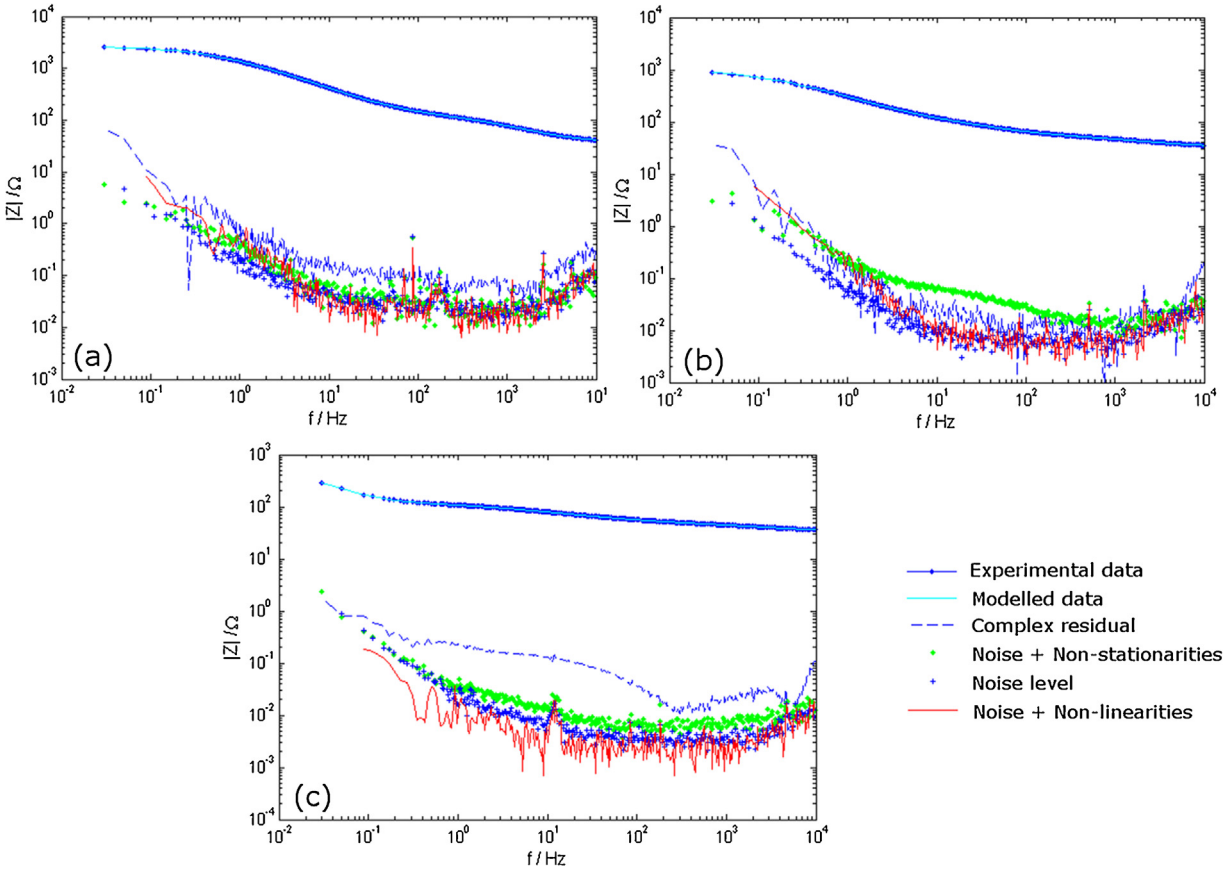

Fig. 4. Experimental and modelled impedance and noise levels of the degradation of the PPy/Fe materials: PPy_1/Fe (a); PPy_2/Fe (b); PPy_2/Fe with diffusion contribution (c).

In the proposed equivalent circuit, R_o corresponds to the sum of the solution and polymer film resistances [39,50]. The time constant CPE_c-R_p corresponds to the polymer/solution interface. It is characterized by R_p, which is the pore resistance, and CPE_c, which represents the constant phase element of the coating. The $CPE_{Fe/IL}$-$R_{Fe/IL}$ component is related to the Fe/IL interface between iron and iron interlayer. The passivation layer, called here interlayer (IL), is formed on the metallic surface prior to the electrodeposition of the PPy on the iron [8,22,28]. It is described by the charge transfer resistance of the dissolution of the passivation layer, $R_{Fe/IL}$, and the constant phase element of the corresponding interface, $CPE_{Fe/IL}$ [24,40]. The $CPE_{PPy/Fe}$-$R_{PPy/Fe}$ corresponds to the reactions between PPy/Fe; $R_{PPy/Fe}$ and $CPE_{PPy/Fe}$ are related to the charge transfer of the reaction between the polymer and the metal.

In the case of the PPy_2 coating, for the measurements after 117 h the proposed EEC insufficiently reflects the measurements. An alternative model is used, where a Warburg element is added in series with the resistance in the $CPE_{PPy/Fe}$-$R_{PPy/Fe}$ subcircuit. The Warburg element accounts for the diffusion of the doped salicylate anions or species formed during the material degradation and its impedance is described by

$$Z_w = \frac{A_w}{(j\omega)^{0.5}}, \tag{1}$$

where A_w is the Warburg coefficient, ω is the angular frequency and j is the imaginary number. This modification is not necessary to model the PPy_1 coating behaviour.

A CPE is commonly employed instead of a pure capacitor to compensate the inhomogeneities and non-ideal capacitive behaviour of conducting polymer modified electrodes [22,25,28,51]. The impedance of a constant phase element Z_{CPE} is formulated with

$$Z_{CPE} = \frac{1}{Q(j\omega)^{\alpha}}, \tag{2}$$

When the exponent α approaches 1, the CPE represents an ideal capacitor and Q corresponds to the capacitance. Here, the α value for CPE_c, $CPE_{PPy/Fe}$ and $CPE_{Fe/IL}$ do not approach 1, which excludes the use of a pure capacitor.

In Fig. 4 it can be seen that the modelled impedance curves match adequately the experimental data for both PPy coatings. Similar results are obtained for all experiments. In order to properly asses the quality of the modelling, the complex residual is compared to the noise level. It can be observed that for both type of coatings, the residual overlaps the noise level almost in the whole frequency range. The model proposed for the last impedance spectra of the PPy_2/Fe system also matches the experiment (Fig. 4c).

The circuit parameters and their standard deviations are determined for every experiment. The relative standard deviations for all parameters are, in general, below 3% and never exceed the 15%. The evolution of the resistive and capacitive parameters over time is presented in Figs. 6–8 with the errors bars representing the parameter standard deviations. The parameter values are given with regard to the geometrical area of the electrode.

Generally all resistances, except $R_{PPy/Fe}$, decrease during the first hours after immersion for both coatings. It is due to the fact that the sample starts to interact with the solution, which penetrates the coating through the pores towards the iron surface [40,45]. This initiates the corrosion processes on the metal. Further on, all resistances evolve differently. The film and solution resistance (R_o),

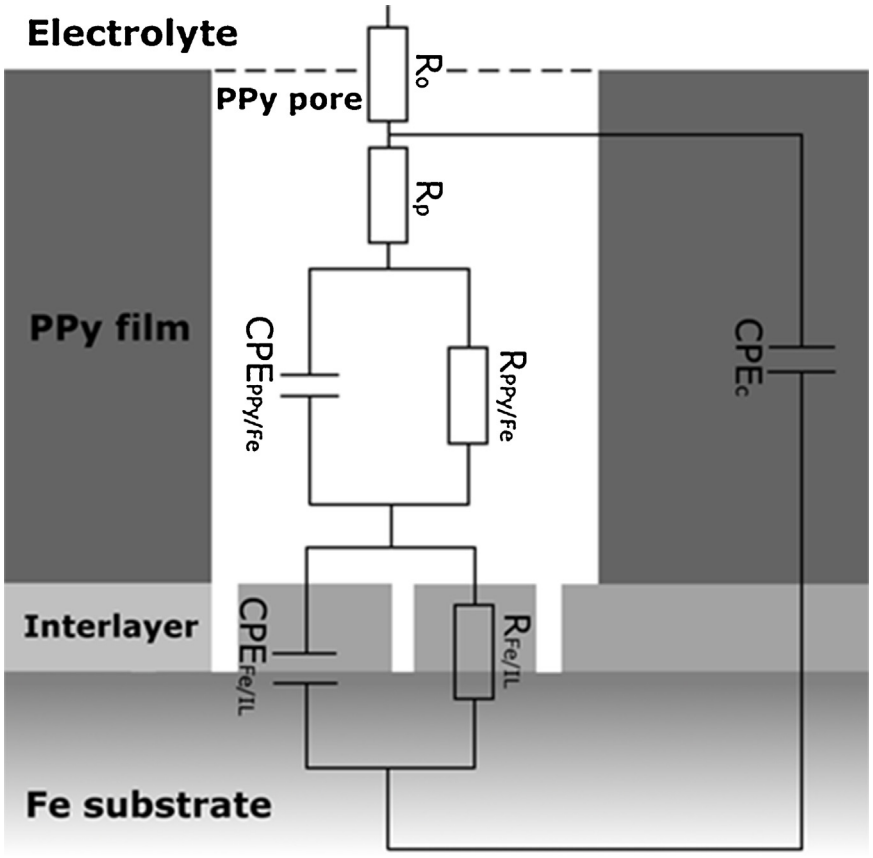

Fig. 5. Equivalent electrical circuit of schematically represented PPy coated iron used to model the EIS data.

for both types of PPy coatings, increase with immersion time (Fig. 6a), indicating that the PPy film is gradually reduced from the electroactive oxidized conducting form to the electro-inactive insulating form [9]. Such behaviour confirms the auto-dedoping model proposed by Beck et al. [52]. They observed that, just after the immersion, the polymer starts to reduce (dedoping process), with a simultaneous release of the anions incorporated into its structure during the electropolymerization. This process was also

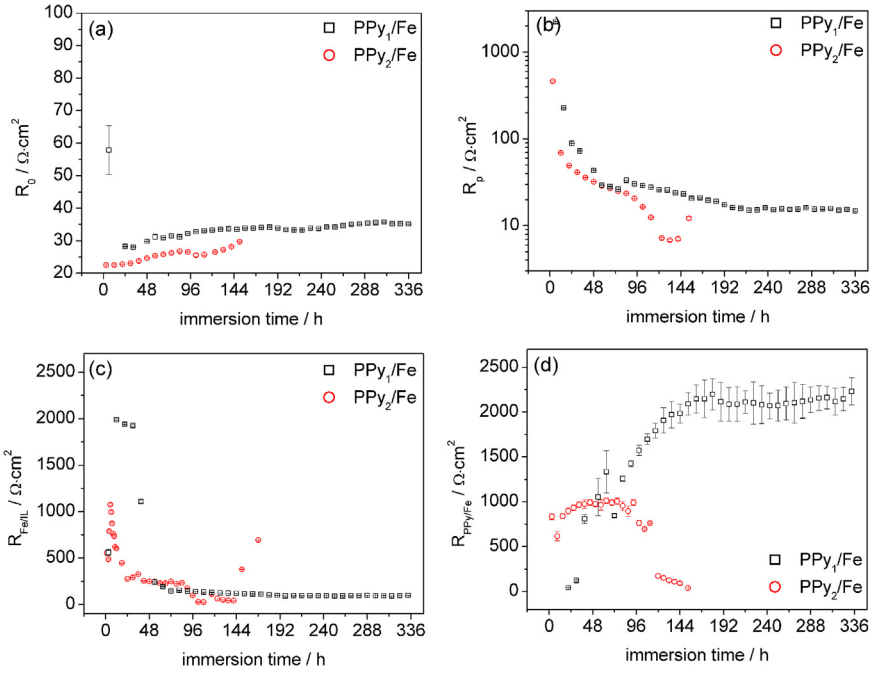

Fig. 6. Evolution of the resistive parameters over time for PPy_1 and PPy_2 coated iron.

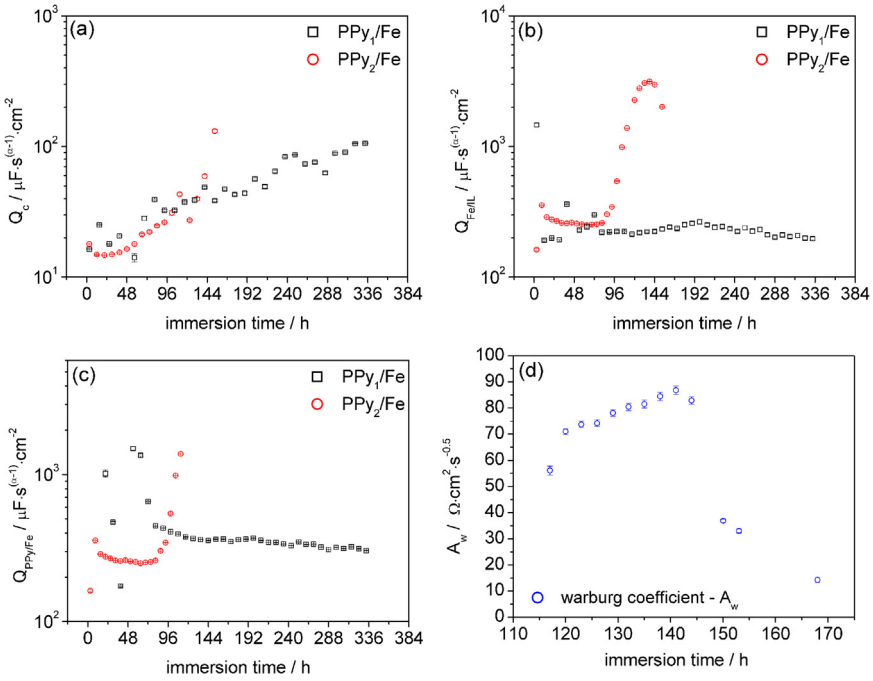

Fig. 7. Evolution of the Q and A_w parameters over time for PPy_1 and PPy_2 coated iron.

noticed by other authors [25,34,39,47]. It also has to be noted that R_o is higher for PPy_1/Fe than for PPy_2/Fe over the whole study, as a consequence of the thicker film.

The rapid decrease of the pore resistance R_p is related to the penetration of the solution into the micropores of the coating [24,39]. Later on, the values of this resistance become constant, reaching a plateau and pseudo-plateau for PPy_1 and PPy_2, respectively. For the PPy_2 coating, this occurs earlier due to the faster ingress of electrolyte, caused by the lower thickness of the film (Fig. 6b). From approximately 96 h the decrease and then increase in R_p for PPy_2 can be observed. These can be due to the diffusion of salicylate anions within the polymeric film, which change the conductivity of the solution in the pores. The coating capacitance Q_c rises regularly with time (Fig. 7a). This is related to the slow and progressive electrolyte uptake by the polymeric film. It can be noticed that the increase is virtually the same for both coatings, which might indicate a similar rate of the solution uptake processes.

As for the $R_{Fe/IL}$-$CPE_{Fe/IL}$ component, in Fig. 6c it can be seen that $R_{Fe/IL}$ for the PPy_1 and PPy_2 coatings diminishes until 72 h and then remains constant. From 144 h, the $R_{Fe/IL}$ for the PPy_2 starts to increase. The decrease of $R_{Fe/IL}$ is associated with the progressive dissolution of the passivation layer by the electrolyte moving towards the Fe surface [24,25]. After certain time, $R_{Fe/IL}$ reaches a stable value (Fig. 6c), likewise $Q_{Fe/IL}$ for PPy_1/Fe (Fig. 7b). On the contrary, the $Q_{Fe/IL}$ value for PPy_2/Fe is nearly constant until approximately 96 h of immersion (Fig. 7b). After this time, an increase is observed, which might be related to the larger active surface due to the breakage of the film. From 144 h a decrease of $Q_{Fe/IL}$ for PPy_2/Fe is observed. The latter and the coincident increase of $R_{Fe/IL}$ could be related to the repassivation of iron.

Regarding the elements that represent the PPy/Fe reactions, the charge transfer resistance $R_{PPy/Fe}$ for the PPy_1 coating rises from the start and, it stabilizes approximately after 144 h. The increase of the charge transfer resistance $R_{PPy/Fe}$ is due to the hindered reaction between the polymer and the metal. For the PPy_2 coating, the resistance slightly increases at the beginning and it quickly reaches a plateau, with a significantly lower value than the steady value of the thicker PPy_1 coating. After 96 h, this resistance starts to decrease.

$Q_{PPy/Fe}$ for PPy_1/Fe increases at the beginning after immersion. Further on, it decreases and remains constant. In the case of the PPy_2 coating, the time to reach the steady value is shorter. Yet, after 60 h $Q_{PPy/Fe}$ rises steeply; this is caused by the swelling of the polymer, which, in turn, enlarges the exposed surface area.

For the PPy_2 coating, from 117 h a Warburg element is added to the EEC to model the diffusion of the doped salicylate anions or corrosion species, such as different kinds of iron oxides and hydroxides. As displayed in Fig. 7d, the Warburg coefficient A_w augments until 150 h. Its increase indicates that the diffusion of the species is inhibited [24]. Further on, the Warburg coefficient drops, as a consequence of the easier diffusion due to the dissolved corrosion products.

For conducting polymers, the use of CPE can be linked to a surface distribution of properties, related to the material roughness and the porosity of the films [22,28,48]. Fig. 8a–c present the α values of CPE_c, $CPE_{Fe/IL}$ and $CPE_{PPy/Fe}$, respectively. In general, the α values correlate with the observed behavior of the corresponding Q parameters (Fig. 7a–c). For the CPE of the coating, α fluctuates between 0.7 and 0.8 for PPy/Fe_1. Higher values of α are found for the thinner PPy_2, yet their values are more scattered. Similarly, Zalewska et al. observed lower values of α_c for thicker PPy films [53]. In the case of the Fe/IL interface, α varies between 0.65 and 0.9 for PPy/Fe_1 and starts to stabilize after 48 h with values around 0.75. Similar values are seen for PPy/Fe_2 until 117 h, when α diminishes to 0.5–0.55, in parallel to the high increase of $Q_{Fe/IL}$ (Fig. 7b). $\alpha_{PPy/Fe}$ shows the largest variations for PPy/Fe_1, particularly before 96 h, as it is also seen for Q (Fig. 7c), and it finally reaches a steady value around 0.82. Values around 0.9 are obtained for PPy/Fe_2 until 96 h, when $\alpha_{PPy/Fe}$ decreases down to 0.65. The decrease of α may indicate an increase of the film microporosity. At the beginning the ingress of solution causes the degradation of the polymeric film, which is seen as a diminution of α. The subsequent increase of this parameter is due to a lower

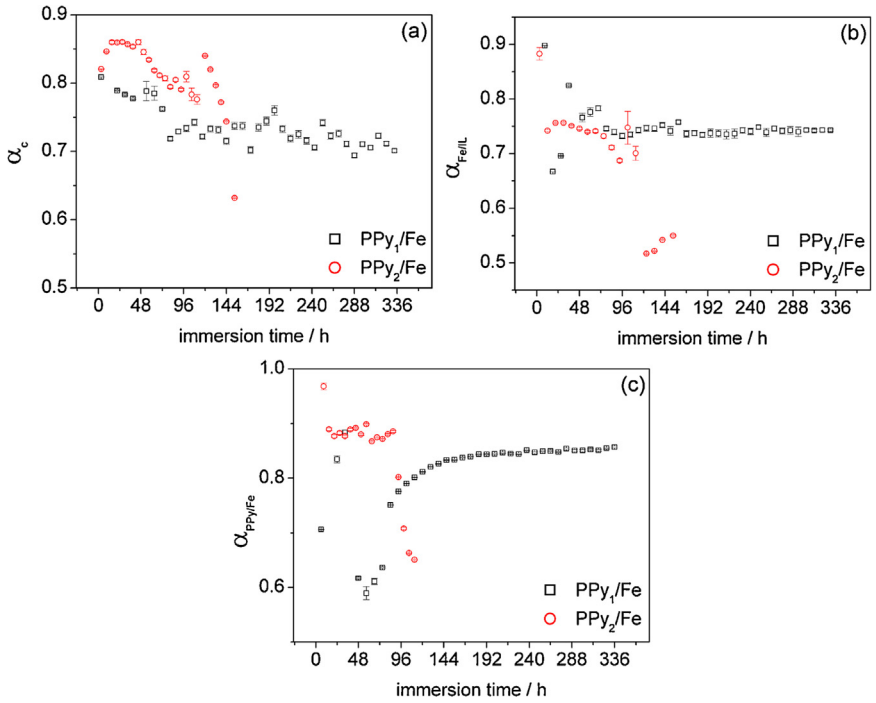

Fig. 8. Evolution of the α parameter over time for PPy_1 and PPy_2 coated iron.

microporosity caused by the expected shrinking of the reduced PPy. A steady value of α is reached due to the deposition of degradation products in the polymer pores.

4. Discussion

The study of two types of PPy coatings with a priori different corrosion properties provides a better understanding of the phenomena and mechanism of electrochemical degradation of iron protected with polypyrrole films. The evaluation of the parameters that describe the impedance experiments indicates that the degradation mechanism occurs in several stages:

- At the beginning, the redox processes occur between PPy and the solution, as it was also reported by other authors [24,25,39]. Because of its electroactive nature, PPy gradually reduces in contact with the solution and salicylate anions are released, according to the following reaction:

$$[PPy^{y+}\,(C_7H_5O_3^-)_y]_n + nye^- \leftrightarrow (PPy)_n + nyC_7H_5O_3^- \quad (1)$$

This can be seen as an increase of R_o, since it includes the film resistance.

- Then the solution penetrates the coating through the pores and the passivation layer formed during the polymerization is progressively dissolved. Subsequently, the electrolyte reaches the iron surface, where active corrosion is initiated; thus $R_{Fe/IL}$ and $R_{PPy/Fe}$ decrease. This process is promoted by the polymer reduction. The degradation of the passivation layer results in the enhancement of the iron degradation, which can be seen in the OCP evolution (Fig. 1). Without the stable passivation layer, the degradation of iron is accelerated. Since the PPy film is porous, less noble Fe substrate corrodes much faster. It is related to the fact that iron exposed at the pores becomes anodic while a vaster area of the PPy film becomes cathodic, leading to localized corrosion [13].

Coinciding with the time when $R_{Fe/IL}$ reaches a constant value, a sudden drop of the OCP occurs. From that moment on, the decomposition of the protective layer results in a lower potential of the coated iron compared to the OCP of bare iron.

- The corrosion process is then inhibited by the formation of corrosion products on the bottom of the film pores. Those are different kinds of iron oxides and hydroxides, which isolate partially the substrate from the corrosive medium [28,32,41,42] (see Supplementary contents, Figure C). Therefore, although the PPy/Fe degradation is first accelerated, it evolves in a steady manner. This effect is confirmed by the stable values of the OCP (Fig. 1) and, in the case of PPy_1/Fe, the α parameters (Fig. 8a–c) as well. Moreover, the deposited iron oxides hinder the electron transfer between the metal and the polymer, with a consequent increase of $R_{PPy/Fe}$ (Fig. 6d).

Therefore, after certain immersion time, the stable degradation is attained for the PPy_1/Fe, which is proved by the evolution of the OCP (Fig. 1) and the circuit parameters (Figs. 6 b–d, 7 b–c, 8 a–c). On the contrary, the stabilization of the PPy_2/Fe system due to the deposition of the corrosion products at the PPy/Fe interface occurs only until a certain immersion time. The charge transfer reaction between the polymer and the iron is inhibited initially; yet, longer immersion causes the anodic dissolution of the newly formed iron oxides, making the corrosion of PPy/Fe proceed [24]. This is seen on the behaviour of $R_{PPy/Fe}$ (Fig. 6d), which is in agreement with the evolution of the OCP (Fig. 1) and the capacitive parameters of the PPy_2/Fe (Figs. 7c and 8c). Later on, the diffusion starts to dominate the electrochemical phenomena at the PPy_2/Fe interface. The mass transport could be related to either the movement of the corrosion products from the iron through the coating [24] or the salicylate ion transport across the PPy film [53]. A diffusion process was observed for poly(o-ethylaniline) coatings on copper after a certain immersion time [24]. Zalewska et al. also reported that only for films thin enough the diffusion processes can be observed [53]. The further immersion leads either to increase of the $R_{Fe/IL}$ (Fig. 6c) or

decrease of $Q_{Fe/IL}$ and A_w (Fig. 7b and d), which could be associated with the repassivation of the iron.

The differences observed in the electrochemical behaviour between the PPy_1 and PPy_2 coatings are due to the film properties, which determine their corrosion performance. The polymer properties can be designed by the electrosynthesis procedure.

The trends in the evolution of the parameters, which are established from the quantitative analysis of the impedance data, describe the stages of the PPy/Fe material. The assessment of the different phases of the material's degradation is based on the reliable EIS modelling. Thus, the current approach provides a solid interpretation of the electrochemistry of PPy coated iron.

From the present study, it can be concluded that a dedicated selection of the polymerization conditions enables engineering the material to have a desired biodegradation rate. Therefore, the degradation of the PPy/Fe material system can be tailored for a possible medical application. PPy is a promising candidate as coating that could first inhibit the corrosion of the metal and then enhance it, with the simultaneous and continuous release of anti-inflammatory salicylates.

5. Conclusions

The degradation of electropolymerized PPy coatings on iron in PBS at 37 °C has been studied by odd random phase electrochemical impedance spectroscopy. It is shown that PPy synthesized from a solution of pyrrole and sodium salicylate can provide the corrosion protection of iron. The modelling with electrical equivalent circuits provides the quantitative description of the electrochemical behaviour. The reliable estimation of the parameters over long term experiments is obtained for the first time. In this way, a solid description of the degradation performance of the PPy/Fe material is attained. It can be concluded that depending on the electropolymerization conditions, and, therefore, on the coating properties, the deterioration of the coated iron evolves differently. Therefore, the degradation of the PPy/Fe material can be tailored by a dedicated design of the electropolymerization procedure. Here, it is found that PPy coatings synthesized under certain conditions inhibit the corrosion of iron at the beginning of the immersion; but later on, they enhance the degradation of the material in a steady manner. This characteristic is very desirable in the case of medical applications, such as biodegradable metallic cardiovascular stents.

Future work will include the study of the salicylate release during the degradation of iron coated with polypyrrole. Also, in-situ ORP-EIS will be conducted during the electropolymerization in order to study the role of the passivation layer in the PPy synthesis on Fe. In the view of a possible medical application, longer degradation study should be also carried out in order to assess how the remaining PPy and its degradation products behave in the long term.

Acknowledgements

This work is supported by a statutory grant for research from the Gdansk University of Technology. The authors would like to thank Priya Laha for the SEM analysis.

Appendix A. Supplementary data

Supplementary data associated with this article can be found, in the online version, at doi; 10.1016/j.electacta.2017.05.172.

References

[1] Y.F. Zheng, X.N. Gu, F. Witte, Biodegradable metals, Mater. Sci. Eng. R 7 (2014) 1.
[2] M. Moravej, D. Mantovani, Biodegradable Metals for Cardiovascular Stent Application: Interests and New Opportunities, Int. J. Mol. Sci. 12 (2011) 4250.
[3] A. Francis, Y. Yuyun, S. Virtanen, A.R. Boccaccini, Iron and iron-based alloys for temporary cardiovascular applications, J. Mater. Sci. – Mater. M 26 (2015) 138.
[4] J. Cheng, T. Huang, Y.F. Zheng, Microstructure, mechanical property, biodegradation behavior, and biocompatibility of biodegradable Fe-Fe2O3 composites, J. Biomed. Mater. Res. A 102A (2014) 2277.
[5] C. Wu, H. Qiu, X.Y. Hu, Y.M. Ruan, Y. Tian, Y. Chu, X.L. Xu, L. Xu, Y. Tang, R.L. Gao, Short-term safety and efficacy of the biodegradable iron stent in mini-swine coronary arteries, Chin. Med. J. 126 (2013) 4752.
[6] D. Sun, Y. Zheng, T. Yin, C. Tang, Q. Yu, G. Wang, Coronary drug-eluting stents: From design optimization to newer strategies, J. Biomed. Mater. Res. A 102 (2014) 1625.
[7] F. Singer, D. Ruckle, M.S. Killian, M.C. Turhan, S. Virtanen, Electropolymerization and Characterization of Poly-N-methylpyrrole Coatings on AZ91D Magnesium Alloy, Int. J. Electrochem. Sci. 8 (2013) 11924.
[8] K. Włodarczyk, F. Singer, P. Jasiński, S. Virtanen, Solid state conductivity of optimized polypyrrole coatings on iron obtained from aqueous sodium salicylate solution determined by impedance spectroscopy, Int. J. Electrochem. Sci. 9 (2014) 7997.
[9] K. Cysewska, S. Virtanen, P. Jasiński, Electrochemical activity and electrical properties of optimized polypyrrole coatings on iron, J. Electrochem. Soc. 162 (12) (2015) E307.
[10] X. Bai, T.H. Tran, D. Yu, A. Vimalanandan, X. Hu, M. Rohwerder, Novel conducting polymer based composite coatings for corrosion protection of zinc, Corr. Sci. 95 (2015) 110.
[11] A. Cook, A. Gabriel, N. Laycock, On the mechanism of corrosion protection of mild steel with polyaniline, J. Electrochem. Soc. 151 (9) (2004) B529.
[12] Y. Luo, X. Wang, W. Guo, M. Rohwerder, Growth behavior of initial product layer formed on Mg alloy surface induced by polyaniline, J. Electrochem. Soc. 162 (6) (2015) C294.
[13] U. Rammelt, P.T. Nguyen, W. Plieth, Corrosion protection by ultrathin films of conducting polymers, Electrochim. Acta 48 (2003) 1257.
[14] P.M. George, A.W. Lyckman, D.A. LaVan, Fabrication and biocompatibility of polypyrrole implants suitable for neural prosthetics, Biomaterials 26 (2005) 3511.
[15] L. Wang, X. Li, Y. Yang, Preparation, properties and applications of polypyrroles, React. Funct. Polym. 47 (2001) 125.
[16] T.V. Vernitskaya, O.N. Efimov, Polypyrrole: A conducting polymer (synthesis, properties, and applications), Russ. Chem. Rev. 66 (1997) 489.
[17] S. Sadki, P. Schottland, N. Brodie, G. Sabouraud, The mechanisms of pyrrole electropolymerization, Chem. Soc. Rev. 29 (2000) 283.
[18] M.C. Turhan, M. Weiser, H. Jha, S. Virtanen, Optimization of electrochemical polymerization parameters of polypyrrole on Mg-Al alloy (AZ91D) electrodes and corrosion performance, Electrochim. Acta 56 (2011) 5347.
[19] T. Tüken, Polypyrrole films on stainless steel, Surf. Coat.Tech. 200 (2006) 4713.
[20] S. Sirivisoot, R. Pareta, T.J. Webster, Electrically controlled drug release from nanostructured polypyrrole coated on titanium, Nanotechnology 22 (2011) 085101.
[21] G. Inzelt, Conducting Polymers, 2nd ed., Springer, 2012.
[22] H. Nguyen Thi Le, B. Garcia, C. Deslouis, Q. Le Xuan, Corrosion protection and conducting polymers: polypyrrole films on iron, Electrochim. Acta 46 (2001) 4259.
[23] K. Cysewska, J. Karczewski, P. Jasiński, Influence of electropolymerization conditions on the morphological and electrical properties of PEDOT film, Electrochim. Acta 76 (2015) 156.
[24] V. Shinde, A.B. Gaikwad, P.P. Patil, Synthesis and corrosion protection study of poly(o-ethylaniline) coatings on copper, Surf. Coat. Tech. 202 (2008) 2591.
[25] A. Yağan, N.Ö. Pekmez, A. Yildiz, Investigation of protective effect of poly(N-ethylaniline) coatings on iron in various corrosive solutions, Surf. Coat. Tech. 201 (2007) 7339.
[26] Z. Grubač, I.Š. Rončević, M. Metikoš-Huković, Corrosion properties of the Mg alloy coated with polypyrrole films, Corros. Sci. 102 (2016) 310.
[27] H. Ryu, N. Sheng, T. Ohtsuka, S. Fujita, H. Kajiyama, Polypyrrole film on 55% Al-Zn-coated steel for corrosion prevention, Corros. Sci. 56 (2012) 67.
[28] V. Annibaldi, A.D. Rooney, C.B. Breslin, Corrosion protection of copper using polypyrrole electrosynthesized from a salicylate solution, Corros. Sci. 59 (2012) 179.
[29] M. Bazzaoui, E.A. Bazzaoui, L. Martins, J.I. Martins, Electrochemical synthesis of adherent polypyrrole films on zinc electrodes in acidic and neutral organic media, Synth. Met. 128 (2002) 103.
[30] F. Beck, R. Michaelis, F. Schloten, B. Zinger, Film forming electropolymerization of pyrrole on iron in aqueous oxalic acid, Electrochim. Acta 39 (1994) 229.
[31] N.T.L. Hien, B. Garcia, A. Pailleret, C. Deslouis, Role of doping ions in the corrosion protection of iron by polypyrrole films, Electrochim. Acta 50 (2005) 1747.
[32] M. Bazzaoui, J.I. Martins, S.C. Costa, E.A. Bazzaoui, T.C. Reis, L. Martins, Sweet aqueous solution for electrochemical synthesis of polypyrrole Part 2. On ferrous metals, Electrochim. Acta 51 (2006) 4516.
[33] L.M. Duc, V.Q. Trung, Layers of inhibitor anion-doped polypyrrole for corrosion protection of mild steel, INTECH 7 (2013) 143.

[34] M.B. González, S.B. Saidman, Corrosion protection properties of polypyrrole electropolymerized onto steel in the presence of salicylate, Prog. Org. Coat. 75 (2012) 178.
[35] M.I. Redondo, C.B. Breslin, Polypyrrole electrodeposited on copper from an aqueous phosphate solution: Corrosion protection properties, Corr. Sci. 49 (2007) 1765.
[36] Y.H. Lei, N. Sheng, A. Hyono, M. Ueda, T. Ohtsuka, Electrochemical synthesis of polypyrrole films on copper from phytic solution for corrosion protection, Corr. Sci. 76 (2013) 302.
[37] M. Bazzaoui, J.I. Martins, T.C. Reis, E.A. Bazzaoui, M.C. Nunes, L. Martins, Electrochemical synthesis of polypyrrole on ferrous and non-ferrous metals from sweet aqueous electrolytic medium, Thin Solid Films 485 (2005) 155.
[38] N.V. Krstajić, B.N. Grgur, S.M. Jovanović, M.V. Vojnović, Corrosion protection of mild steel by polypyrrole coatings in acid sulfate solutions, Electrochim. Acta 42 (1997) 1685.
[39] B.N. Grgur, N.V. Krstajić, M.V. Vojnović, Č. Lačnjevac, Lj. Gajić-Krstajić The influence of polypyrrole films on the corrosion behavior of iron in acid sulfate solutions, Prog. Org. Coat. 33 (1998) 1.
[40] A. Yağan, N.Ö. Pekmez, A. Yildiz, Elecrochemical synthesis of poly(N-methylaniline) on an iron electrode and its corrosion performance, Electrochim. Acta 53 (2008) 5242.
[41] D.E. Tallman, Y. Pae, G.P. Bierwagen, Conducting polymers and corrosion: polyaniline on steel, Corr. Sci. 55 (1999) 779.
[42] D.E. Tallman, Y. Pae, G.P. Bierwagen, Conducting polymers and corrosion: Part 2?Polyaniline on aluminium alloys, Corr. Sci. 56 (2000) 401.
[43] Y.V. Ingelgem, E. Tourwé, O. Blajiev, R. Pintelon, A. Hubin, Advantages of odd random phase multisine electrochemical impedance measurements, Electroanal. 21 (2009) 730.
[44] E. Van Gheem, R. Pintelon, J. Vereecken, J. Schoukens, A. Hubin, P. Verboven, O. Blajiev, Electrochemical impedance spectroscopy in the presence of nonlinear distortions and non-stationary behaviour. Part I: theory and validation, Electrochim. Acta 49 (2004) 4753.
[45] O. Blajiev, R. Pintelon, A. Hubin, Detection and evaluation of measurement noise and stochastic non-linear distortions in electrochemical impedance measurements by a model based on a broadband periodic excitation, J. Electroanal. Chem. 576 (2005) 65.
[46] Impedance Spectroscopy, Emphasizing Solid Materials and Systems, in: J.R. McDonald (Ed.), John Wiley & Sons Inc., 1987.
[47] B.N. Grgur, P. Živković, M.M. Gvozdenović, Kinetics of the mild steel corrosion protection by polypyrrole-oxalate coating in sulphuric acid solution, Prog. Org. Coat. 56 (2006) 240.
[48] G. Bereket, E. Hűr, The corrosion protection of mild steel by single layered polypyrrole and multilayered polypyrrole/poly(5-amino-1-naphtol) coatings, Prog. Org. Coat. 65 (2009) 116.
[49] B. Zeybek, N.Ö. Pekmez, E. Kilic, Electrochemical synthesis of bilayer coatings of poly(N-methylaniline) and polypyrrole on mild steel and their corrosion protection performances, Electrochim. Acta 56 (2011) 9277.
[50] P. Ferloni, M. Mastragostino, L. Meneghello, Impedance analysis of electronically conducting polymers, Electrochim. Acta 41 (1996) 27.
[51] R. Solmaz, Electrochemical synthesis of poly-2-aminothiazole on mild steel and its corrosion inhibition performance, Prog. Org. Coat. 70 (2011) 122.
[52] V. Haase, F. Beck, Electrodeposition of N-substituted polypyrroles on iron and the CIPL strategy, Electrochim. Acta 39 (1994) 1195.
[53] T. Zalewska, A. Lisowska-Oleksiak, S. Biallozor, V. Jasulaitiene, Polypyrrole films polymerised on a nickel substrate, Electrochim. Acta 45 (2000) 4031.